ERROR PROPAGATION IN THE PRODUCTION OF DEM-DOM-DLG BY DIGITAL PHOTOGRAMMETRY

Jingxiong Zhang[a, *], Miao Lu[a], Hao Gong[a], Na Yao[a]

[a]School of Remote Sensing Information Engineering of Geomatic Engineering, Wuhan University, 129 Luoyu Road, Wuhan 43007, - jxzhang@whu.edu.cn

Commission II, WG-II-7

ABSTRACT:

This paper adopts the stochastic simulation method that pertains to geostatistics, on the basis of simulated DEM realizations with spatial autocorrelation errors, to explore the error propagation mechanism of DEM-DON-DLG under the digital photogrammetry environment. It follows this procedure: first, produce 100 error-disturbed DEMs by means of sequential Gaussian simulation; next, attain 100 realizations of DOM based on the digital photogrammetric system VirtuoZo; third, semi-automatically extract some boundaries of land cover to simulate 100 DLGs; last, proceed to perimeter and area error propagation of a number of polygons. Moreover, for comparison, error propagation in polygonal perimeters and areal extents was also performed using the law of variance-covariance propagation. The experiments show that the results of analytical-based error propagation are much lower than the standard deviations of perimeter or area calculated by the stochastic simulation, for the former overlooks the property of spatial autocorrelation and co-relation among variables which objectively exist in the spatial process (including DEM-DOM-DLG error propagation). The research will play a positive role in semi-automatically error processing in the process of digital photogrammetry spatial information acquisition.

1. INTRODUCTION

With the development of surveying and mapping instruments and technology, the technique of aerophotogrammetric mapping has changed from conventional photogrammetry to digital photogrammetry. Based on digital images and the principles of photogrammetry, digital photogrammetry applies computer technology, digital image processing, image matching, pattern recognition and so on to extract digital-represented geometrical and physical information of objects. The differences between conventional photogrammetry and digital photogrammetry are that the products, intermediate data records and source data of the latter are all in digital form. The whole process is executed based on computers and corresponding softwares.

The basic data provided by aerophotogrammetry and remote sensing includes digital elevation models (DEMs), digital orthophoto models (DOMs) and digital line graphs (DLGs). Based on the digital photogrammetric system VirtuoZo, the constitution of DEM is to project the parallax grid to the earth coordinate system to create irregular grid, according to the parallax data of image matching, orientation elements and corresponding parameters. And then a regular grid DEM is founded by interpolation methods and so on. DOM, based on the DEM data, are produced by digital rectification according to the inverse solution。After data acquisition and editing applied to objects in stereo images or a DOM, the attained three-dimensional digital map file is exported as vectorgraph, the so-called DLG, according to standard cartographic symbols. Through the work flow mentioned above, it is not uneasy to conclude that if a DEM is accompanied with errors, then it will no doubt affect the accuracy of the following DOM and DLG.

At present, researches on the accuracy and quality control of DEM, DOM and DLG each are comparatively abroad (McIntosh and Krupnik, 2002; Simon and Harvey 2004; Amnon Krupnik 2003; Y.D. Huang 2000). However, little work has been carried out to investigate the error propagation among the three. This paper adopts the stochastic simulation method to create error-disturbed DEMs, produces corresponding DOMs, analyzes polygon perimeter and area error propagation based on DLGs attained semi-automatically and reveals the characteristic of the error propagation of DEM-DOM-DLG.

2. SOURSE OF ERROR AND ERROR PROGATION

During the production process based on the digital photogrammetric system, DEM is the realization base of the DOM and DLG production. The basic procedure of generating DEM described here is related to scanned aerial stereo images. The idea can also be applied to other types of image obtained from an aerial camera or satellite sensor. In the platform of VirtuoZo, the workflow of DEM production is shown in Figure 1.

As is shown above, the accuracy of DEM depends on the following factors: scan quality of original images, orientation accuracy of digital model, terrain feature and matching editing.

Based on DEM, the generation process of DOM consists of three steps: digital differential, digital mosaic and map sheet clipping and decoration. The paper concerns the error of digital differential, without considering the importance of the errors produced by the other two steps. The essential of digital

differential is geometry transformation between two images, in which inverse resolution is more widely used. As for each pixel of the orthophoto, its corresponding ground coordinates are firstly calculated and then the image coordinates are calculated by the collinearity equations:

$$x - x_0 = -f\frac{a_1(X - X_s) + b_1(Y - Y_s) + c_1(Z - Z_s)}{a_3(X - X_s) + b_3(Y - Y_s) + c_3(Z - Z_s)} \left.\begin{matrix} \\ \\ \end{matrix}\right\}$$
$$y - y_0 = -f\frac{a_2(X - X_s) + b_2(Y - Y_s) + c_2(Z - Z_s)}{a_3(X - X_s) + b_3(Y - Y_s) + c_3(Z - Z_s)} \left.\begin{matrix} \\ \\ \end{matrix}\right\} \qquad (1)$$

The image grey value is sequentially calculated by interpolation based on the image coordinates and the interpolated grey value is assigned to the pixel.

The accuracy of DEM impacts the generation of DOM. On one hand, the elevation value of each pixel in orthophoto is extracted from DEM. On the other hand, as shown in Equation (1), elevation value Z obtained by DEM interpolation will affect the image coordinate calculation.

There are three methods to generate DLG, that is digital photogrammetry, scanning vectorization and vectorization of DOM. With the development of high-resolution satellite and remote sensing image softwares, the third method whereby to generate corresponding DLG based on possessed DOM has been an economical and effective way.

The same characteristic of the first and third methods is that DOM is the base map used to extract and edit object feature. Hence, when DOM is contaminated by errors, it will propagate the errors to DLG inevitably.
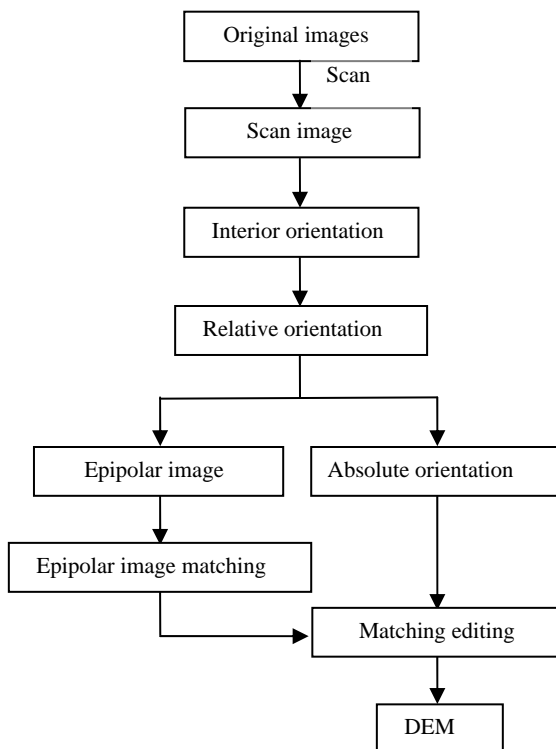
```
Original images
      │ Scan
      ▼
Scan image
      │
      ▼
Interior orientation
      │
      ▼
Relative orientation
      │
      ├──────────────────┐
      ▼                  ▼
Epipolar image    Absolute orientation
      │                  │
      ▼                  │
Epipolar image matching  │
      │                  │
      └──────► Matching editing ◄──┘
                  │
                  ▼
                 DEM
```

Figure 1. Work flaw of DEM production

Through the analysis above, it is clear that the DEM, DOM and DLG error propagation process during the practical work will undoubtedly influences the quality of DEM, DOM and DLG. Therefore, an alternative approach is required to analyze the error propagation. This paper adopts random simulation method to simulate the random error of DEM, generates DOM in digital photogrammetric system consequently, semi-automatically extracts some boundaries to simulate DLG, and finally applies analytical method to analyze error propagation quantitatively. The random simulation method and analytical approach of error propagation will be depicted in detail as follows.

3. RANDOM SIMULATION METHOD OF ERROR PROPAGATION

Implementation of the sequential principle under the multiGaussian Random Function (RF) model is referred to as sequential Gaussian simulation (sGs). The algorithm is widely used, especially applied to continuous variable satisfied Gaussian distribution.

Consider the simulation of the continuous attribute z at N nodes $x_j{}'$ of a grid conditional to the data set $\{z(x_a), a = 1, \cdots, n\}$.

Sequential Gaussian simulation proceeds as follows:
a)   The first step is to check the appropriateness of the multiGaussian RF model, which calls for a prior transform of z-data into y-data with a standard normal cumulative distribution function (cdf) using the normal score transform.
b)   If the multiGaussian RF model is retained for the y-variable, sequential simulation is performed on the y-data:
   • Define a random path visiting each node of the grid only once.
   • At each node x', determine the parameters (mean and variance) of the Gaussian cumulative conditional distribution function (ccdf) using Simple Kringing (SK) with the normal score semivariogram model. The conditioning information consists of a specified number of both normal score data and values simulated at previously visited grid nodes.
   • Draw a simulated value from that ccdf, and add it to the data set.
   • Proceed to the next node along the random path, and repeat the two previous steps.
   • Loop until all N nodes are simulated.
c)   The final step consists of back-transforming the simulated normal scores $\{y^{(l)}(x_j'), j = 1, \cdots, N\}$ into simulated values for the original variable, which amounts to applying the inverse of the normal score transform to the simulated y-value.

Other realizations $\{z^{(l')}(x_j'), j = 1, \cdots, N\}, l' \neq l$, are obtained by repeating steps 2 and 3 with a different random path.

In this paper, realizations of 100 error DEMs is based on sGs algorithm and error DEM layer is achieved by subtracting the two original DEMs which refer to reference DEM and error DEM. Some ground points are selected in the region to calculate variogram of the error DEM layer, because sGs strongly depends on variogram. Firstly, perform normal score transform of elevation error data. And then, build variogram model with sill value and range as input parameters for sGs. Afterwards, according to sGs, 100 realizations of error DEM layers are obtained. Error DEM layers are superimposed on the

reference DEM and 100 error DEMs are realized consequently (shown in Figure 2).
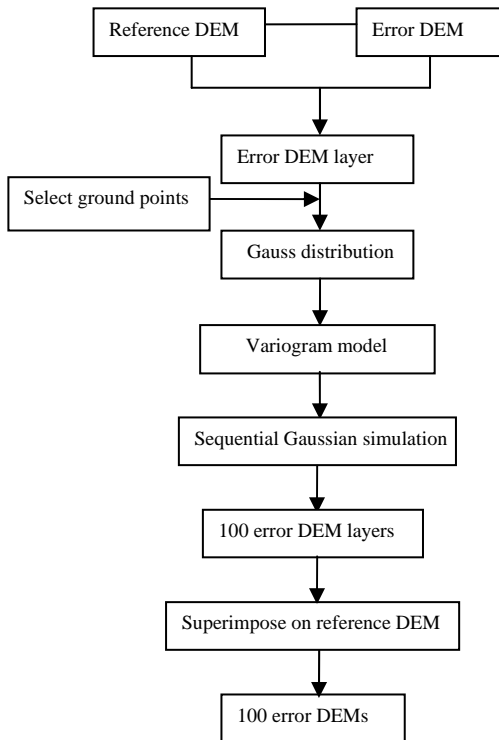

Figure 2.Work flow of 100 error DEM realizations

4. ANALYTICAL APPROACH OF ERROR PROPAGATION

Based on the 100 error DEMs and reference DEM, using digital photogrammetric system, the corresponding DOMs can be attained respectively. After that, the land cover boundaries, which can be regarded as a series of polygons composed of polylines, are semi-automatically extracted from the DOMs in order to obtain the realizations of DLG. As for the reference DLG, analytical method of error propagation is adopted. The principle is that the variances of length and area rely on the quantification and incorporation of spatial correlation in positional errors, which will be described below.

Consider polyline objects that are sequences of line segments connecting vertices. Then, it is possible to sum the lengths of individual line segments to obtain the length of a polyline. If a polyline links three vertices (points) x_1, x_2, and x_3, it is straightforward to calculate its lengths as the sum of Euclidean distance $\|x_2 - x_1\|$ and $\|x_3 - x_2\|$. One can differentiate polyline length, $\|x_2 - x_1\| + \|x_3 - x_2\|$, which respect to X_1, Y_1, X_2, Y_2, X_3, and Y_3 as:

$$
\begin{aligned}
d(length) = & \|x_2 - x_1\|^{-1}\left(-\Delta X_1 dX_1 - \Delta Y_1 dY_1\right) \\
& + \left(\|x_2 - x_1\|^{-1}\Delta X_1 - \|x_3 - x_2\|^{-1}\Delta X_2\right) dX_2 \\
& + \left(\|x_2 - x_1\|^{-1}\Delta Y_1 - \|x_3 - x_2\|^{-1}\Delta Y_2\right) dY_2 \\
& + \|x_3 - x_2\|^{-1}\left(\Delta X_2 dX_3 + \Delta Y_2 dY_3\right)
\end{aligned}
\tag{2}
$$

Where ΔX_i and ΔY_i stand for the shifts of X and Y coordinates form point x_i to points x_{i+1}, that is, $(\Delta X_i, \Delta Y_i)^T = x_{i-1} - x_i$.

Assume non-zero covariances between X and Y coordinates at individual points, and between X or Y coordinates in immediately neighboring points such as x_1 and x_2, or x_2 and x_3. Then, on the basis of Equation (1), it is possible to derive the variance of polyline length from:

$$
\begin{aligned}
\text{var}(length) = & \|x_2 - x_1\|^{-2}\begin{bmatrix}\Delta X_1^2(\sigma_{X_1}^2 - 2\sigma_{X_1X_2} + \sigma_{X_2}^2) + 2\Delta X_1\Delta Y_1(\sigma_{X_1Y_1} + \sigma_{X_2Y_2}) \\ + \Delta Y_1^2(\sigma_{Y_1}^2 - 2\sigma_{Y_1Y_2} + \sigma_{Y_2}^2)\end{bmatrix} \\
& + \|x_3 - x_2\|^{-2}\begin{bmatrix}\Delta X_2^2(\sigma_{X_2}^2 - 2\sigma_{X_2X_3} + \sigma_{X_3}^2) + 2\Delta X_2\Delta Y_2(\sigma_{X_2Y_2} + \sigma_{X_3Y_3}) \\ + \Delta Y_2^2(\sigma_{Y_2}^2 - 2\sigma_{Y_2Y_3} + \sigma_{Y_3}^2)\end{bmatrix} \\
& - 2\|x_2 - x_1\|^{-1}\|x_3 - x_2\|^{-1}\begin{bmatrix}\Delta X_1\Delta X_2(\sigma_{X_2}^2 - \sigma_{X_1X_2} - \sigma_{X_2X_3}) \\ + \Delta Y_1\Delta Y_2(\sigma_{Y_2}^2 - \sigma_{Y_1Y_2} - \sigma_{Y_2Y_3}) \\ + (\Delta X_1\Delta Y_2 + \Delta X_2\Delta Y_1)\sigma_{X_2Y_2}\end{bmatrix}
\end{aligned}
\tag{3}
$$

Where $\sigma_{X_1}^2$, $\sigma_{Y_1}^2$, $\sigma_{X_2}^2$, $\sigma_{Y_2}^2$, $\sigma_{X_3}^2$, $\sigma_{Y_3}^2$, $\sigma_{X_1X_2}$, $\sigma_{Y_1Y_2}$, $\sigma_{X_2X_3}$, $\sigma_{Y_2Y_3}$, $\sigma_{X_1Y_1}$, $\sigma_{X_2Y_2}$, and $\sigma_{X_3Y_3}$ stand for the variances and covariances of the X and Y components of the positional errors at or between the points as identified by the subscripts.
Equation (3) includes many covariance components for a simple polyline consisting of three vertices. It can be further expanded into a polyline object comprised n vertices. At the same time, assume zero spatial correlation in positional errors among neighboring points, plus uniformity in X and Y variance and zero XY covariance, then simplification is as following:

$$
\begin{aligned}
\text{var}(length) = & 2(n-1)\sigma^2 - \\
& 2\sum_{i=1}^{n-2}\|x_{i+1} - x_i\|^{-1}\|x_{i+2} - x_{i+1}\|^{-1}(\Delta X_i\Delta X_{i+1} + \Delta Y_i\Delta Y_{i+1})\sigma^2
\end{aligned}
\tag{4}
$$

Consider now the case of area measurements of polygons. A combination of differentiation and variance propagation leads to the evaluation of variance in area estimation. Consider a polygon consisting of a sequence of vertices that are traversed counter-clockwise. Then, the areal extent of the polygon is calculated as a positive sum of vector products. The differential of the area of a polygon consisting of n vertices is given by:

$$
d(area) = \frac{1}{2}\sum_{i=1}^{n}\left[(Y_{i+1} - Y_{i-1})dX_i - (X_{i+1} - X_{i-1})dY_i\right]
\tag{5}
$$

Where (X_i, Y_i) stand for the X and Y coordinates of the i th vertex numbered in a circular fashion.
Based on the equation (4), area variance is computed by propagation of the variances in positional errors of the component vertices of the polygon as:

$$\mathrm{var}(area) = \frac{1}{4}\sum_{i=1}^{n}\begin{bmatrix} \Delta Y_{i+1}^2 \sigma_{X_i}^2 + \Delta X_{i+1}^2 \sigma_{Y_i}^2 - 2\Delta X_{i+1}\Delta Y_{i+1}\sigma_{X_i Y_i} \\ +2\Delta Y_i \Delta Y_{i+1}\sigma_{X_i X_{i+1}} + 2\Delta X_i \Delta X_{i+1}\sigma_{Y_i Y_{i+1}} \end{bmatrix} \qquad (6)$$

Where $\sigma_{X_i}^2$, $\sigma_{Y_i}^2$, $\sigma_{X_i Y_i}$, $\sigma_{X_i X_{i+1}}$, and $\sigma_{Y_i Y_{i+1}}$ stand for the variances and covariances of the X and Y components of the positional errors at the vertices, and column vectors $(\Delta X_i, \Delta Y_i)^T = x_{i+1} - x_{i-1}$, and $(\Delta X_{i+1}, \Delta Y_{i+1})^T = x_{i+2} - x_i$, representing the shifts of X and Y coordinates between specified points.

Assuming zero spatial correlation between neighboring vertices defining the polygon's boundaries, plus uniform variances in X and Y coordinates but zero covariance, Equation (4) can be simplified to:

$$\mathrm{var}(area) = \frac{1}{4}\sum_{i=1}^{n}(\Delta Y_{i+1}^2 + \Delta X_{i+1}^2)\sigma^2 = \frac{1}{4}\sum_{i=1}^{n}l_{i+2,i}^2 \sigma^2 \qquad (7)$$

Where $l_{i+2,i}$ is the distance between the $(i+2)$th and ith vertexes, which impacts the area variance. At the same time, variances of X and Y coordinates affect the value of var*(area)*.

5. EXPERIMENTAL RESULT AND ANALYSIS

This experiment selected a pair of aerial stereo images in a certain area of Xianning, Hubei province. The 1:4,000 scale photographs were flown with a camera of focal length of 153.82 mm and at a flight height of 3125 m. They were scanned at a resolution of 0.025 mm.

Based on the digital photogrammetric system VirtuoZo, a reference DEM and error DEM were generated with the former meeting the standard of practical production according to the work flow shown in Figure 1 and the latter accompanied by some errors. And then according to the flow chart in Figure 2, 100 error DEMs were realized by sGs algorithm. Moreover, variogram model with the parameters 1.0 Gau(30.0) was fitted with 169 elevation error values of ground points selected in the study region. Based on the variogram model, the SGSIM module of GSLIB was run to get 100 realizations of error DEM, and 100 DOMs can be generated with respect to those DEMs using VirtuoZo system. Obvious differences are shown between the reference DOM and error DOM in Figure 3.

ArcGIS was run to implement the vectorization of DOMs for the production of DLGs. According to the types of land covers, the region was mainly divided into six areas: cultivated Land (area 1), forest land (area 2), exposed field (area 3), habitation (area 4), factories (area 5) and ponds (area 6)(shown in Figure 4). Whereafter, some feature points were selected from the boundaries of the areas in each DOM. The routes of the vectorization were along the same boundaries and passed through these points. Figure 5 shows 100 simulated realizations of DLG superimposed on the reference DOM.

Feature 3(a). A subregion of the reference DOM

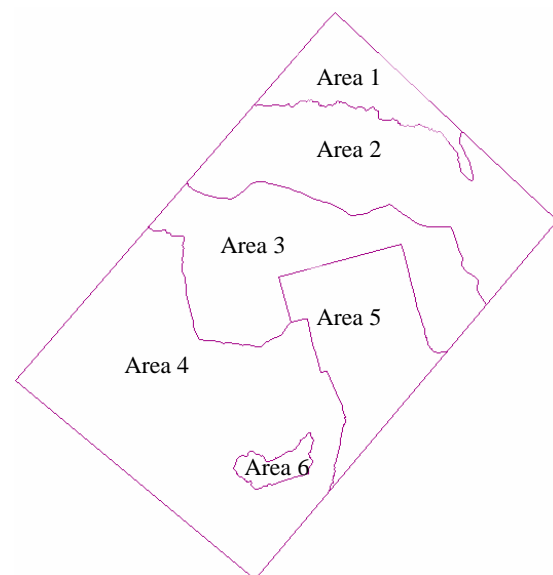Feature 3(b). Corresponding subregion of the error DOM

Figure 4. The boundaries of land covers

Figure 5. 100 simulated DLGs overlaid on reference DOM

Based on the error DLGs, areas and perimeters of every polygon formed with boundaries were calculated. And then the standard deviation of 100 DLGs were obtained by mathematical statistics (in Table 1)

Area	1	2	3	4	5	6
$\sigma(area)$	160.103	257.818	200.807	362.882	192.132	145.901
$\sigma(perimeter)$	18.874	20.940	9.804	14.351	8.988	11.173

Table 1. Area and perimeter standard deviations of 100 DLGs

For the reference DLG, standard deviations of area and perimeter were computed by the analytical approach of error propagation. Since the accuracy of the original DEM is credible, the position errors of points were assumed to be the size of a pixel, that is to say, 0.1 confirmed by the image scale and scan resolution. According to Equations (4) and (7), the perimeter and area standard deviations of the reference DLG were calculated without considering spatial correlation between neighboring vertices which defined the polygon's boundaries. The results are shown in Table 2.

Area	1	2	3	4	5	6
$\hat{s}(area)$	27.309	27.397	23.133	39.370	30.134	3.096
$\hat{s}(perimeter)$	0.856	0.924	0.605	0.703	0.638	0.822

Table 2. Area and perimeter standard deviations of the reference DLG

The corresponding scatter diagrams of area and perimeter are shown in Figure 6 where the dashed lines and the solid lines respectively stand for standard deviation values of the error DLGs and the reference DLG. It is clear that standard deviations of the error DLGs is larger than those of the reference DLG, for the spatial correlation of position error is not taken into account.
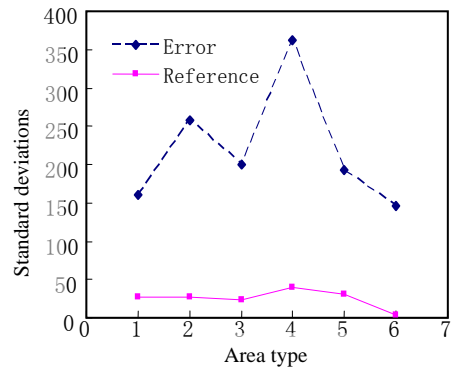

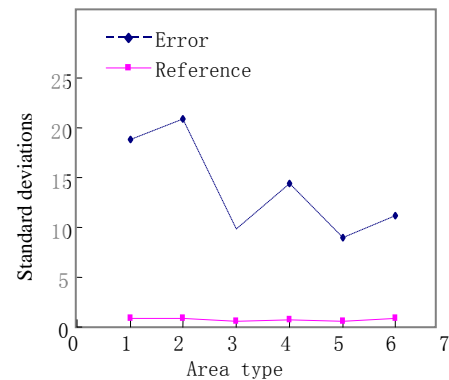Figure 6(a) Scatter diagram of area standard derivations

Figure 6(b) Scatter diagram of perimeter standard deviations

According to Charles Ghilani's (2000, 60(3), p.177-182) research result about error propagation, it is shown that the number of points formed polygon impacts the accuracy of value calculated by simple computational method. If the points are much more and denser, the value will be smaller compared with the approach considering spatial correlation. There were more than 200 points in every vectorization boundary of the simulated DLGs, so the spatial correlation among the points, especially adjacent point was larges. Whereas, if covariances were not considered, it will greatly influence the result value. As is shown in scatter diagrams, standard deviation values of the reference DLG are much smaller than those of the error DLGs.

6. CONCLUSION

This paper has demonstrated the potential of stochastic simulation for tracking and quantifying error propagation digital photogrammetry as an alternative to analytical approaches, which are based on Taylor series expansion and variance and covariance propagation. As stochastic simulation can furnish error modelling with spatial correlation taken into account, it is theoretically more rigorous than the analytical approaches, whose implementation is usually reduced to assuming zero spatial covariance, thus subject to biases in error statistics. Experiments with quantifying error statistics in polygonal perimeters and areas suggest that there is a huge difference between standard deviations calculated from vector map realizations digitized based on realized DOMs and those by analytical approaches, especially with respect to polygons

with more sampled points. Error statistics in areas see less discrepancy than those in perimeters.

It was hypothesized that errors in photogrammetric vector data result from those originating in semi-automatic image matching, which can be emulated by adding error surfaces onto DEMs whereby error-contaminated DEMs will lead to distorted DOMs from which vector data are extracted. In an operational setting for digital photogrammetry, a semi-automatic process of error propagation may be implemented if geostatistical procedures for variogram modelling, conditional simulation, post-processing, and visualization can be incorporated into the photogrammetry workstation. However, it is also important to recognize that geostaistics may be new to general photogrammetrists. Thus, user interface design is a necessity along with wider use of geostatistics.

It may be of further interests to investigate the (lack of) commonality between error propagation in point-fixing by land surveying and that in digital photogrammetry. The error statistics reported in this paper show increased discrepancies between those obtained by simulation vs. those by analytical simplification as opposed to what was reported in Ghilani (2000). One explanation may be the greater numbers of points involved in digitizing in digital photogrammetry than those in land surveying. However, there may be something enlightening in surveying adjustment for photogrammetricts to ponder upon.

REFERENCE

Amnon, K., 2003. Accuracy prediction for ortho-image generation. *Photogrammetric Record*, 18(101), pp. 41-58.

Ghilani, D., 2000. Demystifying Area Uncertainty: More or Less. *Surveying and Land Information System*, 60 (3), pp. 177-182. http://surveying.wb.psu.edu/psu-surv/Chuckbio.htm

McIntosh, K. and Krupnik, A., 2002. Integration of laser-derived DSMs and matched image edges for generating an accurate surface model. *ISPRS Journal of Photogrammetry & Remote Sensing*, 56(3), pp. 167-176.

Pierre, G., 1997. *Geostatistic for natural resources elevation.* Oxford, New York, pp. 380-392.

Simon, B. and Hervey, M., 2004. Integration, validation and point spacing optimisation of digital elevation models. *Photogrammetric Record,* 19(108), pp. 277-295.

Y. D. Huang, 2000. Evaluation of information loss in digital elevation models with digital photogrammetric systems. *Photogrammetric Record*, 16(95), pp. 781-791.

Zhang, J. and Goodchild, M.F., 2002. Uncertainty in Geographical Information. London and New York: Taylor & Francis.

ACKNOWLEDGEMENTS